Available online at www.sciencedirect.com
SCIENCE DIRECT
Electrochimica Acta 51 (2006) 1960–1966
ELECTROCHIMICA Acta
www.elsevier.com/locate/electacta

Investigation of cobalt deposition using the electrochemical quartz crystal microbalance

J.T. Matsushima, F. Trivinho-Strixino, E.C. Pereira *

Centro Multidisciplinar para o Desenvolvimento de Materiais Cerâmicos, Laboratório Interdisciplinar de Eletroquímica e Cerâmica, Departamento de Química, Universidade Federal de São Carlos, Caixa Postal 676, São Carlos 13565-905, SP, Brazil

Received 8 December 2004; received in revised form 21 March 2005; accepted 2 July 2005
Available online 3 August 2005

Abstract

Electrodeposition of cobalt from sulfate solutions at different pH values was investigated using the EQCM technique coupled with cyclic voltammetry. The results show that cobalt hydroxide is formed simultaneously with cobalt deposition during the early stages of reduction due to the pH variation near the electrode surface caused by the parallel hydrogen evolution reaction (HER). This result was confirmed using M/z values calculated using the Sauerbrey equation and Faraday's law, which showed the presence of cobalt hydroxide in the electrodeposits. A flux model was developed and it assumes a direct reduction of cobalt, simultaneous HER and the formation of cobalt hydroxide during the early stages of deposition at pH 4.10. When the solution pH is decreased to 3.33 only the direct cobalt reduction is observed without any hydroxylated species formation.

Keywords: Electrodeposition; Quartz crystal microbalance; pH effect; Cobalt; Cobalt hydroxide

1. Introduction

Cobalt is an important metal due to its use in magnetic alloys, cutting-wear resistant alloys and super alloys [1,2]. Recently, electrodeposited Co and Co alloys have been investigated with the aim of optimizing experimental conditions to obtain films with magnetic properties and the usage in magnetic storage systems [3–7]. The magnetic properties depend on the morphology and microstructure of the Co deposits [4,5]. As the morphology and microstructure of the films can be controlled by the preparation parameters (e.g. solution composition, applied potential, current density, additives and pH [8–11]), the electrodeposition process can be used to prepare thin films for magnetic applications.

During the electrodeposition of Co the hydrogen evolution reaction (HER) occurs as a side reaction that consumes part of the applied current and reduces the current efficiency and also affects the pH at the electrode surface, modifying the kinetics of metal reduction [12–14]. The increase of pH at the electrode surface can result in the precipitation of cobalt hydroxide, which interferes with the formation of the metallic deposit and a porous metallic structure is produced [8–10]. Consequently, greater understanding of the HER mechanism and control of its kinetics would allow the preparation of Co deposits that are suitable for different applications.

Several mechanisms for cobalt electrodeposition have been proposed in the literature [9–11,15,16]. For some authors [15,16] the cobalt electrodeposition mechanism is thought to occur via the formation of $CoOH^+$ and $Co(OH)_2$ species. The formation of the hydroxide species depends on the pH of the deposition bath. For solution pH lower than 4.0, the authors [15,16] proposed that Co^{2+} and OH^- react producing $CoOH^+$ "unstable complex". The reaction that follows is the reduction of this complex and its reaction with adsorbed hydrogen to form metallic Co. For solution pH between 4.0 and 4.5, the authors [15,16] proposed that Co^{2+} and OH^- reacts producing cobalt hydroxide. This compound is reduced to produce metallic Co. According to the

* Corresponding author. Tel.: +55 16 3351 8214/213; fax: +55 16 3351 8214/208.
E-mail address: decp@power.ufscar.br (E.C. Pereira).

0013-4686/$ – see front matter © 2005 Elsevier Ltd. All rights reserved.
doi:10.1016/j.electacta.2005.07.003

authors, the last reaction involving the reduction of adsorbed hydroxide causes the increase of OH^- concentration near the electrode which changes the surface pH. According to the authors, since OH^- is formed during Cobalt reduction, at pH 4.0 and 4.5, this mechanism does not result in hydrogen evolution.

On the other hand, Jeffrey et al. [11] proposed an alternative mechanism involving $CoOH^+$ ions, whereas the authors do not mention if these ions are free or adsorbed on the electrode. Furthermore, the authors did not consider the dissociation constant of those ions under their experimental conditions, leaving their proposed mechanism very unpredictable. For example, Jeffrey et al. [11] suggested that the limiting step for their proposed mechanism is the reduction of CoOH (an unpredictable species) to metallic Co. Furthermore, the authors did not mention how these particularly unstable species were formed. It has also be shown [9,10] different proposed mechanisms for cobalt electrodeposition considering different reaction paths that involve the formation of cobalt hydroxides and oxides species, or unstable cobalt complex ions, as prior products before effective deposition of metallic cobalt.

Considering the mechanisms described above, sometimes showing the presence of unstable species or unpredictable ions, for the current experimental procedure, we present in this paper a study aiming the usage of the electrochemical quartz crystal microbalance (EQCM) technique simultaneously with cyclic voltammetry in order to compare past results and to propose a practical and alternative mechanism for cobalt electrodeposition at different pH unbuffered solutions. It is proposed that only two different reactions, i.e. direct cobalt reduction and cobalt hydroxide formation, describe the current process without further intermediates. The last reaction is a consequence of the parallel HER. A flux model considering these proposals was made and fitted the data.

2. Experimental

The electrochemical measurements were carried out in a glass cell. The working electrode (WE) was a 9 MHz AT-cut quartz crystal coated with a Pt film in contact with the electrolyte ($A = 0.2\,cm^2$). The sensitivity of the EQCM used was 770 Hz μg^{-1}. The counter electrode (CE) was a Pt sheet and all potentials are referred to saturated calomel electrode (SCE). The resonance frequency shift was measured with a Seiko EG&G quartz crystal microbalance (model QCA 917). The electrochemical measurements were conducted using an EG&G PAR 263A potentiostat/galvanostat.

Cobalt was deposited at $T = 25\,^{\circ}C$ under potentiodynamic conditions on the Pt coated quartz crystal electrode using 0.1 mol L^{-1} $CoSO_4{\cdot}5H_2O$ and 1.53 mol L^{-1} Na_2SO_4 as supporting electrolyte at different pH values (4.10 and 3.33). The pH was adjusted by the addition of 0.1 mol L^{-1} H_2SO_4. All solutions were prepared with deionized water and analytical grade reagents. The potential scan rate was set at $10\,mV\,s^{-1}$.

3. Results and discussion

3.1. Theory

The EQCM technique combined with cyclic voltammetry is a convenient method to investigate electrochemical reactions by measuring the simultaneous current, charge and related mass changes at the working electrode [17]. According to the Sauerbrey equation [18] the frequency variation (Δf) of the quartz crystal is correlated with the mass variation of the electrode (Δm) and can be written as:

$$\Delta f = \frac{-2 f_0^2 \Delta m}{A\sqrt{\mu_i \rho_i}} = -K\,\Delta \mathrm{m} \tag{1}$$

where f_0 is the resonant frequency of the quartz crystal, A the piezoelectric active area, μ_i the shear modulus of the quartz, K the experimental mass coefficient and ρ_i is the density of quartz.

When Eq. (1) is combined with the Faradays law, the number of electrons involved in the reaction can be calculated [18–20].

The species involved in electrochemical reactions on the substrate can be evaluated by plotting the quartz crystal frequency variation (Δf) as a function of the charge consumed during the reaction (Q) according to the equation:

$$\Delta f = -\left(\frac{KM}{Fz}\right) Q \tag{2}$$

where M is the molar mass of the deposit, F the Faraday constant and z is the number of electrons. Rearranging Eq. (2), M/z can be determined by fitting the slope of the mass versus charge curves:

$$\frac{M}{z} = \left|\frac{\mathrm{d}\Delta f}{\mathrm{d}Q}\right| \left(\frac{F}{K}\right) \tag{3}$$

The M/z value combines the Δf and Q data into a single factor that can be used to discuss the reaction mechanism in a simple manner. The corresponding value can be easily calculated for any electrochemical reaction and it indicates if there is a single reaction or several parallel reactions occurring at the electrode surface.

Many authors [21–23] have used the ion flux as a function of potential calculated from EQCM experiments to investigate reaction mechanisms. Following the same procedure, the study of the electroreduction/electrodissolution mechanism of Co using flux analysis is proposed here.

As discussed in the introductory part, Jeffrey et al. [11], Pradhan et al. [15] and Cui et al. [16] cited different mechanisms related to Co electrodeposition in which deposition proceeds through formation of $CoOH^+$ or $CoOH^+$ and $Co(OH)_2$. At low pH values it was proposed that formation

of adsorbed hydrogen occurs. At pH values between 4 and 4.5, the formation of unstable cobalt species, which may be the rate-limiting step, is proposed. However, for the purpose of elaborating a mathematical flux model, it is assumed that only the direct reduction of cobalt takes place, as shown by the equation below:

$$Co^{2+}_{(aq)} + 2e^- \rightarrow Co_{(s)} \quad (4)$$

On the other hand, during metal electrodeposition from aqueous solution at negative potentials, the parallel reaction of water electrolysis occurs. Such a reaction can be related to the formation of cobalt hydroxide as shown below:

$$2H_2O + 2e^- \rightarrow H_{2(g)} + 2OH^-_{(aq)} \quad (5)$$

$$Co^{2+}_{(aq)} + 2OH^-_{(aq)} \rightarrow Co(OH)_{2(s)} \quad (6)$$

Summarizing, Eqs. (5) and (6) are related to the formation of $Co(OH)_2$, while Eq. (4) is related to the direct deposition of cobalt. Cobalt hydroxide reduction requires a much more negative potential than direct cobalt reduction [9].

Thus, considering that Eqs. (4)–(6) occur simultaneously, the mass balance as a function of the applied potential for cobalt electrodeposition at the working electrode is:

$$\Delta m_{(E)} = \sum_i n_i M_{i(E)} = n_{Co^{2+}} M_{Co^{2+}(E)} + n_{Co(OH)_2} M_{Co(OH)_2(E)} \quad (7)$$

The inclusion of water molecules (solvent) to the total mass balance is not suitable in this case, considering the experimental conditions described here. None of the calculated data (Tables 1–4) showed M/z values related to water molecules separately ($M/z_{(H_2O)} = 9$, considering 2 electrons). Furthermore, the overall Faradaic reaction is due to reactions described in Eqs. (4)–(6), and therefore the overall mass variation masks, if it exists, a variation of mass related only to water molecules. The participation of solvent molecules is important in conducting polymers or polyelectrolytes redox processes [24–26] once the solvated counter ions intercalate (or desintercalate) in the polymer matrix. Besides, for double layer structure investigation [27] or monolayers adsorption [28], the contribution of H_2O molecules is important. In these case, the adsorbed solvent molecules must be displaced to accommodate the adsorbed layer. Then, the calculated M/z change account for both processes: the mass increase due to the adsorption of the molecules minus the mass contribution from the displaced adsorbed solvent molecules. For metals deposition, considering that the quantity of atoms deposited is much more than one monolayer, the contribution of the displacement of the solvent (water) molecules from the interface, when the first deposition layer occurs, is negligible compared to the overall mass change.

The charge balance as a function of the applied potential in this process is related to the number of moles of ionic species and can be written as:

$$Q_{(E)} = -\sum_i z_i F n_{i(E)} = -2n_{Co^{2+}} F_{(E)} + 2n_{OH^-} F_{(E)} \quad (8)$$

where F is the Faraday constant. The charge balance is in accordance with the reduction/dissolution of 1 mol of Co and

Table 1
M/z found by fitting the slope of the mass vs. charge for cobalt deposition in the cobalt sulfate solution at pH = 4.10

pH	Potential range (V)[a]	M/z (g mol^{-1})
4.10	(a) −0.80 to −0.84	47.6 ± 0.5
	(a) −0.84 to −0.85	47.5 ± 0.5
	(a) −0.85 to −0.86	43.0 ± 0.5
	(a) −0.86 to −0.87	40.7 ± 0.5
	(a) −0.87 to −0.88	38.2 ± 0.5
	(a) −0.88 to −0.89	35.6 ± 0.5
	(a) −0.89 to −0.90	32.5 ± 0.5
	(b) −0.90 to −0.85	29.0 ± 0.5
	(b) −0.85 to −0.80	29.3 ± 0.5
	(b) −0.80 to −0.65	29.7 ± 0.5

[a] Potential range used for calculate the M/z values obtained for cobalt deposition region: (a) scan toward negative potential and (b) scan toward positive potential after potential inversion at −0.90 V.

Table 2
M/z found by fitting the slope of the mass versus charge for cobalt dissolution in the cobalt sulfate solution at pH = 4.10

pH	Potential range (V)[a]	M/z (g mol^{-1})
4.10	−0.65 to −0.47	28.5 ± 0.5
	−0.47 to −0.41	27.8 ± 0.5
	−0.41 to −0.36	28.1 ± 0.5
	−0.36 to −0.32	29.0 ± 0.5
	−0.32 to −0.29	30.8 ± 0.5
	−0.29 to −0.27	33.4 ± 0.5
	−0.27 to −0.24	38.4 ± 0.5
	−0.24 to −0.23	42.4 ± 0.5
	−0.23 to −0.18	50.4 ± 0.5
	−0.18 to +0.40	39.7 ± 0.5

[a] Potential range used for calculate the M/z values obtained for cobalt dissolution region.

Table 3
M/z found by fitting the slope of the mass versus charge for cobalt deposition in the cobalt sulfate solution at pH = 3.33

pH	Potential range (V)[a]	M/z (g mol^{-1})
3.33	(a) −0.89 to −0.90	28.3 ± 0.5
	(a) −0.87 to −0.88	30.6 ± 0.5
	(a) −0.89 to −0.90	29.7 ± 0.5
	(b) −0.86 to −0.84	29.0 ± 0.5

[a] Potential range used for calculate the M/z values obtained for cobalt deposition region: (a) scan toward negative potential and (b) scan toward positive potential after potential inversion at −0.90 V.

Table 4
M/z found by fitting the slope of the mass versus charge for cobalt dissolution in the cobalt sulfate solution at pH = 3.33

pH	Potential range (V)[a]	M/z (g mol^{-1})
3.33	−0.52 to −0.21	29.6 ± 0.5

[a] Potential range used for calculate the M/z values obtained for cobalt dissolution region.

with the electrolysis of 1 mol of H_2O. It is assumed that only Faradaic electrochemical processes occur.

Considering the simultaneous reaction of water electrolysis and Co^{2+} reduction, it can be proposed that the amount of generated OH^- is directly proportional to the amount of $Co(OH)_2$ formed, according to Eqs. (5) and (6). Now, if it is considered that $Co(OH)_2$ formation is generated from water electrolysis and proceeds at 100% efficiency in the early stages of electrodeposition, the charge balance as a function of the applied potential can be written as:

$$Q_{(E)} = -\sum_i z_i F n_{i(E)} = -2n_{Co^{2+}} F_{(E)} + 2n_{Co(OH)_2} F_{(E)} \quad (9)$$

Rearrangement of Eqs. (7) and (9) has an analytical solution, since there are two equations and two variables. Considering this, from Eqs. (7) and (9), the number of $n_{Co^{2+}}$ and $n_{Co(OH)_2}$ species can be calculated as a function of the applied potential (E):

$$n_{Co^{2+}(E)} = \left(\Delta m_{(E)} - \frac{Q_{(E)} M_{Co(OH)_2}}{2F}\right)\beta \quad (10)$$

$$n_{Co(OH)_2(E)} = \left(\Delta m_{(E)} + \frac{Q_{(E)} M_{Co^{2+}}}{2F}\right)\beta \quad (11)$$

where β is:

$$\beta = \frac{1}{M_{Co^{2+}} + M_{Co(OH)_2}}$$

By differentiation of Eqs. (10) and (11) with respect to time, the species flux as a function of the current density and mass flux, is obtained:

$$\frac{dn_{Co^{2+}(E)}}{dt} = \left(\frac{d(\Delta m_{(E)})}{dt} - \frac{i_{(E)} M_{Co(OH)_2}}{2F}\right)\beta \quad (12)$$

$$\frac{dn_{Co(OH)_2(E)}}{dt} = \left(\frac{d(\Delta m_{(E)})}{dt} + \frac{i_{(E)} M_{Co^{2+}}}{2F}\right)\beta \quad (13)$$

As a convention, positive flux values indicate deposition and negative values indicate dissolution or ejection of the ionic species.

3.2. Deposition and dissolution of cobalt

Fig. 1 shows the cyclic voltammogram and the mass variation as a function of potential for cobalt electrodeposition at pH 4.10. The cobalt reduction begins at −0.8 V and it is accompanied by a mass increase that indicates Co deposition on the electrode. After reversing the potential at −0.9 V, the cobalt reduction proceeds up to −0.66 V. Between this potential and −0.60 V the mass of the electrode remains constant where no Faradaic reaction occurs. Two crossovers between cathodic current branches are observed during the scan toward positive potential. The more cathodic crossover (−0.85 V) corresponds to the nucleation overpotential from

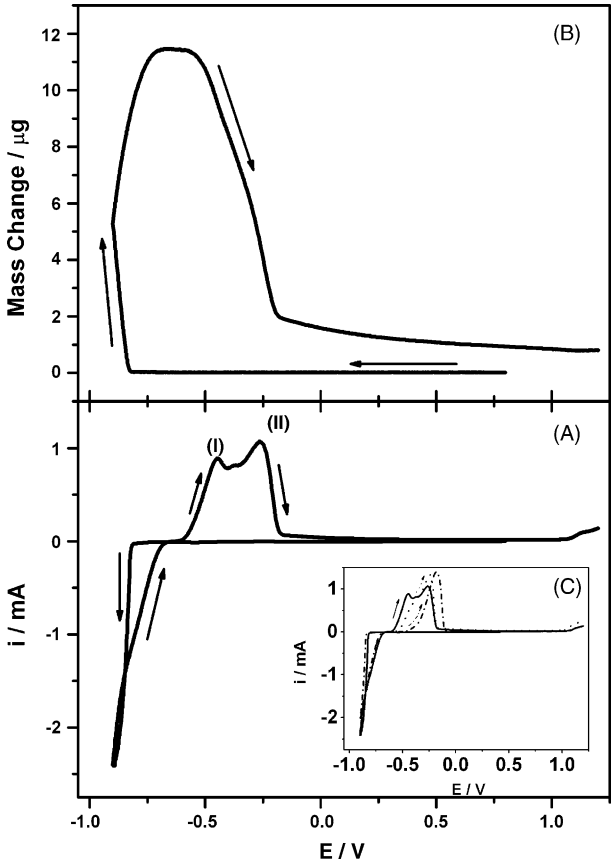

Fig. 1. (A) Cyclic voltammograms and (B) mass variation as a function of potential measured in a solution containing 0.1 M $CoSO_4$; 1.53 M Na_2SO_4 at pH 4.10 for cobalt electrodeposition. (C) Cyclic voltammograms at different polarization times for cobalt electrodeposition: 15 min (- - -), 60 min (. . . .).

which the parameters of the nucleation-growth mechanism are taken [29]. The second crossover was observed at −0.66 V and corresponds to the crossover potential. At potentials more negative than −0.85 V, the current for the scan toward positive potential is lower than that before the inversion of potential (−0.90 V), probably due to the corresponding change in the concentration of $Co(H_2O)_6^{2+}$ ions at the electrode surface [29], due to the deposition process. On the other hand, in the range between −0.85 and −0.66 V, the current toward positive potential scan was higher than before the inversion of potential. According to this, as expected, it can be concluded that the energy required for cobalt deposition on the cobalt film, during the forward sweep, is lower than that required for cobalt deposition on the bare Pt electrode.

At more anodic potentials the cobalt dissolution process begins at −0.60 V which is characterized by both an anodic current peak and a mass decrease on the electrode. Two current peaks were observed at −0.45 V (process I) and −0.27 V (process II) in Fig. 1A. These processes can be related to the HER that occurs simultaneously with cobalt reduction (Eq. (4)). According to Soto et al. [29], processes I and II could be related either to the dissolution of cobalt from electrode into the solution in form of different ionic species or to the disso-

lution of different cobalt phases that were previously formed during the cathodic sweep.

In order to understand the results shown in Fig. 1 and to evaluate the mechanism of cobalt deposition in these experiments an analysis of the pH of the deposition bath and working electrode polarization time was carried out.

Different polarization times at −0.64 V (Fig. 1C) were investigated to characterize the dissolution peaks observed in Fig. 1A. As can be seen in the inset, the potential peak related to process I vanishes as the polarization time increases, while displacement toward positive potentials of the potential peak related to process II is observed, which can now be associated with the dissolution of cobalt without adsorbed hydrogen. Since the greater part of the chemisorbed hydrogen is formed during the HER side reactions, this hydrogen rich phase is formed during cobalt reduction, as [12]:

$$H_3O^+ + e^- + Co \rightarrow CoH_{(ads)} + H_2O \quad (14)$$

$$H_3O^+ + CoH_{(ads)} + e^- \rightarrow H_{2(ads)} + H_2O \quad (15)$$

$$H_{2(ads)} \rightarrow H_{2(g)} \quad (16)$$

Eq. (14) refers to the discharge of H_3O^+ ions initially located in the Outer Helmhotz Plane, while Eqs. (15) and (16) are related to the electrochemical dessorption and diffusion of adsorbed hydrogen molecules from the electrode surface. Although we did not observe bubbles formation over the electrode and considering that process I disappear when the electrode is polarized, we believe that this process can be associated with the dissolution of hydrogen rich cobalt phase. For Ni deposits, it is proposed [30–32] the formation of a nickel hydride phase. In the case of Co, to our knowledge, there is not any experimental evidence of the formation of a CoH phase. Our results indicate that at least a hydrogen rich cobalt phase is formed under the investigated conditions.

Using the M/z values determined by the slope of the fitting mass data as a function of charge, all species involved during Co electrodeposition process, studied at different values of solution pH, can be visualized. Table 1 shows the M/z values calculated from experiments carried out at pH 4.10 for deposition and dissolution of Cobalt. In the initial stages of cobalt reduction, the calculated M/z value is 46.6 g mol^{-1}, which is compatible with $Co(OH)_2$ species and in accordance with Eqs. (5) and (6) where two electrons are involved ($MW_{Co(OH)_2}/2e^-$). As the potential is displaced toward more negative values, M/z decreases close to the theoretical value predicted for direct cobalt reduction (MW = 29.5 g mol^{-1}) at −0.86 V, just after the inversion of potential. In this potential range it is suggested that direct Co^{2+} reduction occurs (Eq. (4)), as mentioned earlier.

For Co dissolution, M/z values correspond only to pure Cobalt dissolution (Table 2). $Co(OH)_2$ species were also detected for potentials more positive than 0.25 V during a short range of potentials (Table 2). We can compare the same potential range in Tables 1 and 2 with the data presented in Fig. 1, where the current density decreases after process II.

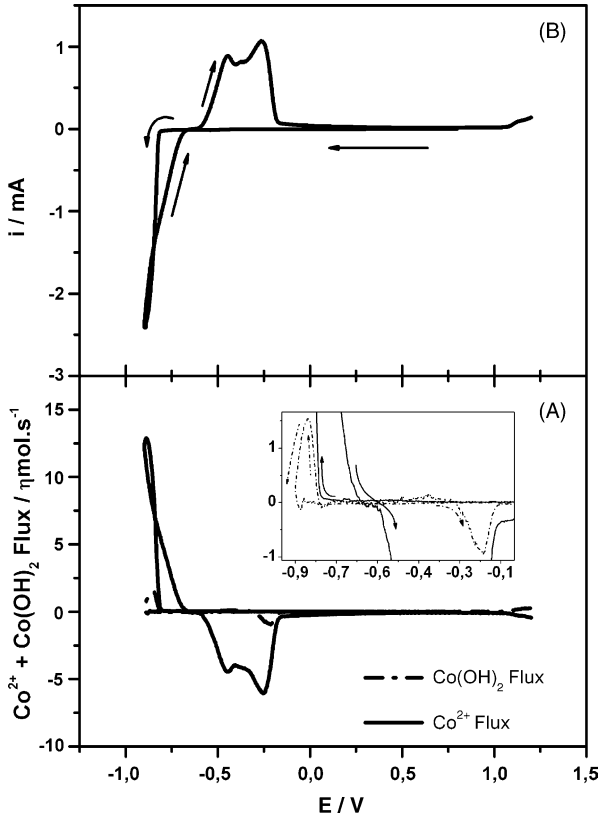

Fig. 2. (A) Flux of Co and $Co(OH)_2$ as a function of potential and (B) cyclic voltammogram measured in a solution containing 0.1 M $CoSO_4$; 1.53 M Na_2SO_4 at pH 4.10 for cobalt electrodeposition.

Consequently, the remaining current and mass variation after this potential can be related to the dissolution of cobalt and cobalt hydroxide that had been previously deposited simultaneously on the electrode surface.

The flux of Co and $Co(OH)_2$ during the cobalt electrodeposition at pH 4.10 can be calculated from the EQCM and voltammetry data, according to Eqs. (12) and (13) (Fig. 2). The Co reduction begins at a −0.8 V, the same potential range where $Co(OH)_2$ was detected (Table 1), indicating a simultaneous deposition of these species. Nakahara and Mahajan [8] reported the same behavior for cobalt electrodeposition on a sheet of annealed copper. At −0.86 V, $Co(OH)_2$ reaches the maximum flux value and coincides with the same potential where the experimental M/z value is compatible with $Co(OH)_2$ species (46.6 g mol^{-1}) (Table 1). At this point it is assumed that the formation of Cobalt hydroxide in the vicinity of the electrode ceases or its rate decreases and the remaining current is used in a direct deposition of Co^{2+}. After this potential, the flux of cobalt hydroxide begins to decrease until reaching zero (Fig. 2), where at −0.9 V only Co species were detected (29 g mol^{-1}) as can be seen in Table 1. The dissolution of the cobalt hydroxide is observed at the end of process II, in conjunction with the dissolution of Co^{2+}. Similar results were observed by Soto et al. [29] using the same voltammetric technique and the deposition and dissolution of

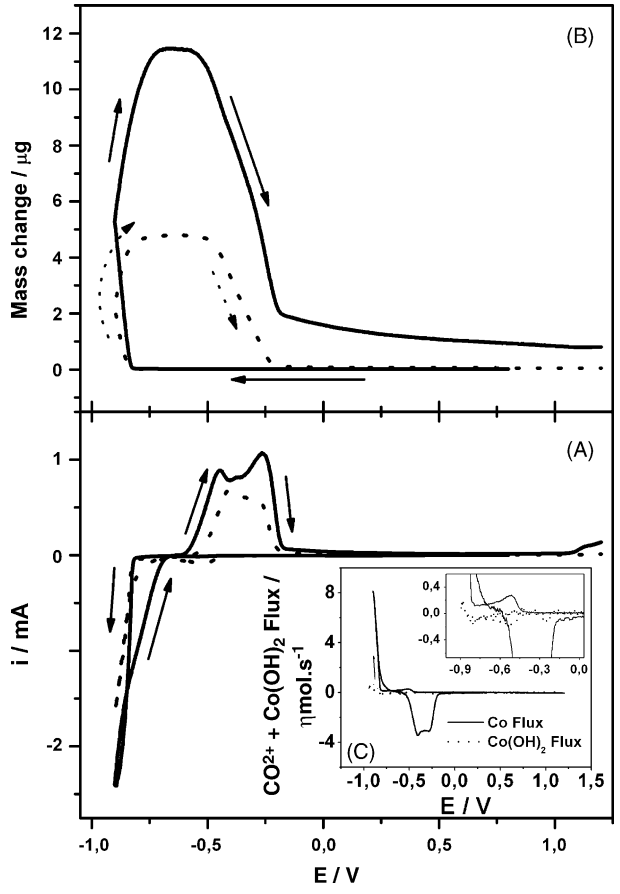

Fig. 3. (A) Cyclic voltammograms and (B) mass variations as a function of potential measured in a solution containing 0.1 M $CoSO_4$; 1.53 M Na_2SO_4 at pH 4.10 (—) and 3.33 (....) adjusted with H_2SO_4. (C) *Inset*: flux of Co and $Co(OH)_2$ as a function of potential measured in a solution containing 0.1 M $CoSO_4$; 1.53 M Na_2SO_4 at pH 3.33.

Co and $Co(OH)_2$ occur simultaneously [8] at the beginning and end of the process, respectively.

For experiments carried out at pH 3.33 (Fig. 3), a decrease in the mass change is observed probably due to the increasing effect of the HER, which decreases the Co deposition efficiency [8]. After this, the mass variation at the end of deposition returns to the same value as at the beginning, while for a solution of pH 4.10 the mass variation was not reversible. However, cobalt hydroxide was not detected as illustrated by the data in Tables 3 and 4, where no M/z values for $Co(OH)_2$ are observed. The absence of hydroxide species can be related to the decreasing amount of free OH^- ions reacting with Co^{2+} in the vicinity of the electrode surface, leading to direct Co deposition (Eq. (4)).

The flux curve, in this case, indicates only the existence of Co^{2+} instead of Co^{2+} and $Co(OH)_2$ during the electrodeposition process (Fig. 3C). The deviation for small flux values is inside the error expected considering the procedure of calculation and the sensibility of the quartz crystal microbalance during electrodeposition at pH 3.33 (inset in Fig. 3C).

Finally, it is important to stress that the interpretation given above in correct only if the surface roughness does not change during the experiments [27]. We believe, that this parameter, surface roughness, indeed does not change due to: (a) in the present case, the cobalt deposit thickness is only 67 nm (deposited mass = 12 μg, Cobalt density = 8.9 g cm^{-3}, electrode area = 0.2 cm^2). Therefore, it is not expected that a change in the roughness factor occurs during the experiment. (b) Besides, a signature of a change in the electrode area is a loop during the reduction process, i.e. at the same potential, the current observed during the sweep towards the negative direction is lower than those observed during the sweep towards positive potentials. In Figs. 1 and 3, it is clear that the loop is absent for the experiment done at both pH investigated. Then, we conclude that the roughness factor is constant during our experiments.

4. Conclusions

The analysis of the EQCM data during cobalt electrodeposition points to the formation of cobalt hydroxide during deposition. The absence of cobalt hydroxide in the experiments carried out at pH 3.33 was also confirmed. This result was confirmed by both the M/z values and flux model analyses. The deposition of cobalt was accompanied by the HER and the results indicates that at least an hydrogen rich cobalt phase is formed under the investigated conditions, as confirmed by polarization experiments. Cobalt hydroxide is formed due to variation of solution pH (>4.10) and the formation of hydroxide ions at the electrode surface caused by the HER. The EQCM technique combined with cyclic voltammetry was found to be a useful in situ tool for investigating the effects of pH and polarization time on the electrode surface during metal deposition.

Acknowledgement

The authors are grateful to FAPESP and CNPq (Brazil) for the financial support.

References

[1] F.R. Morral, in: M.G. Howe (Ed.), Othmer-Kirk-Encyclopedia of Chemical Technology, vol. 5, John Wiley & Sons, New York, 1964, p. 716.
[2] D. Landolt, Eletrochim. Acta 39 (8–9) (1994) 1075.
[3] B. Brozzini, D. De Vita, A. Sportoreletti, G. Zangari, P.L. Cavalloti, J. Magn. Magn. Mater. 120 (1993) 300.
[4] T. Osaka, Electrochim. Acta 42 (1997) 3015.
[5] S. Armyanov, Electrochim. Acta 45 (2000) 3323.
[6] P.L. Cavalloti, N. Lecis, H. Fauster, A. Ziclonka, J.P. Celis, G. Wantas, J. Machado da Silva, J.M. Brochado Oliveira, M.A. Sá, Surf. Coat. Technol. 105 (1998) 232.
[7] J.L. Su, M.M. Chen, J. Lo, R.E. Lee, J. Appl. Phys. 63 (1988) 4022.
[8] S. Nakahara, S. Mahajan, J. Electrochem. Soc. 127 (1980) 283.
[9] S.P. Jiang, Y.Z. Chen, J.K. You, T.X. Chen, A.C.C. Tseung, J. Electrochem. Soc. 137 (1990) 3374.

[10] S.P. Jiang, A.C.C. Tseung, J. Electrochem. Soc. 137 (11) (1990) 3387.
[11] M.I. Jeffrey, W.L. Choo, P.L. Breuer, Miner. Eng. 13 (2000) 1231.
[12] D.R. Gabe, J. Appl. Electrochem. 27 (1997) 908.
[13] Ph. Vermeiren, R. Leysen, H. Vandendorre, Electrochim. Acta 30 (1985) 1253.
[14] A. Zhou, N. Xie, J. Colloid Interface Sci. 220 (1999) 281.
[15] N. Pradhan, T. Subbaiah, S.C. Das, J. Appl. Electrochem. 27 (1997) 713.
[16] C.Q. Cui, S.P. Jiang, A.C.C. Tseung, J. Electrochem. Soc. 137 (1990) 3418.
[17] D.A. Buttry, in: H.D.A. Armario (Ed.), Electrochemical Interfaces: Modern Techniques for in situ Interface Characterization, VHC, New York, 1991 (Chapter 10).
[18] H. Saloniemi, M. Kemel, M. Ritala, M. Leskelä, J. Electroanal. Chem. 482 (2000) 139.
[19] J.G.N. Matias, J.F. Julião, D.M. Soares, A. Goresnstein, J. Electroanal. Chem. 431 (1997) 163.
[20] A. Marlot, J. Vedel, J. Electrochem. Soc. 146 (1999) 177.
[21] A.R. Hillman, Solid State Ionics 94 (1997) 151.
[22] S.L.A. de Maranhão, R.M. Torresi, Electrochim. Acta 44 (1999) 1879.
[23] H. Varela, M.R. Torresi, J. Electrochem. Soc. 147 (2000) 665.
[24] H. Varela, M. Malta, R.M. Torresi, J. Power Source 92 (2001) 50.
[25] H. Varela, S.L.A. de Maranhão, R.M.Q. Mello, E.A. Ticianelli, R.M. Torresi, Synth. Met. 122 (2001) 321.
[26] A. Jackson, A.R. Hillman, S. Bruckenstein, I. Jureviciute, J. Electroanal. Chem. 524–525 (2002) 90.
[27] V. Tsionsky, G. Katz, E. Gileadi, L. Daikhin, J. Electroanal. Chem. 524–525 (2002) 110.
[28] Z. Jusys, S. Bruckenstein, Electrochem. Commun. 2 (2000) 412.
[29] A.B. Soto, E.M. Arce, M. Palomar-Pardave, I. González, Electrochim. Acta 41 (1996) 2647.
[30] M. Fleishmann, A. Saraby, Electrochim. Acta 29 (1984) 69.
[31] Y.P. Lin, J.R. Selman, J. Electrochem. Soc. 140 (1993) 1299.
[32] H. Hayashi, S. Matsuda, Electrochemistry 70 (2002) 768.